Chapter 1

Basic physical principles of body diffusion-weighted MRI

Eric E. Sigmund and Jens Jensen

1.1 Introduction

The possibility of sensitizing nuclear magnetic resonance (NMR) signals to molecular diffusion was recognized in the early, pioneering days of NMR by Hahn[1], Carr and Purcell[2]. In the 1960s, the Stejskal–Tanner pulse sequence for measuring diffusion properties was introduced and has been a mainstay of diffusion NMR every since[3–4]. The Stejskal–Tanner sequence is also the prototypical pulse sequence for diffusion-weighted imaging (DWI), although for human imaging there are a number of variants and alternative sequences that help manage the practical challenges of clinical scanning.

Until recently, DWI in humans has been dominated by brain applications, to a large degree because the relatively long transverse relaxation times (T2) in the brain help maintain a sufficient signal-to-noise ratio (SNR) and the good field homogeneity helps minimize imaging artifacts. However, recent improvements in scanning hardware and pulse sequence design have now made feasible good quality DWI for the body, and body applications are becoming increasingly common[5–6].

In this chapter, we review the basic physical principals of DWI, emphasizing issues particularly pertinent to body applications. We begin with diffusion NMR physics, covering both the relevant concepts of molecular diffusion and the essential theory for the Stejskal–Tanner pulse sequence. We will consider practical aspects of image acquisition, such as sequence selection and artifact reduction. The analysis of DWI data and an overview of selected important body applications will be discussed.

1.2 Diffusion NMR physics

Molecules within a liquid move in a complicated pattern that can be regarded as a random process. This process may be quantified by various types of probability distributions – the most commonly used being the probability $P(\mathbf{r}, t)$ of a molecule moving a displacement vector $\mathbf{r}$ in a time t. For DWI, the molecule of interest is generally water.

Since the total probability of moving some amount is always unity, we have the normalization condition

$$\int d^3 r P(\mathbf{r}, t) = 1. \tag{1.1}$$

The mean or average value of an arbitrary function $F(\mathbf{r})$ is simply given by

$$\langle F(\mathbf{r}) \rangle \equiv \int d^3 r P(\mathbf{r}, t) F(\mathbf{r}), \tag{1.2}$$

with the angle brackets being a shorthand for the average.

The molecular motion in a particular direction $\mathbf{n}$ ($|\mathbf{n}| = 1$) is conveniently characterized by the "moments":

$$M_i(\mathbf{n}) \equiv \left\langle (\mathbf{r} \cdot \mathbf{n})^i \right\rangle, \tag{1.3}$$

where i is a positive integer. In equilibrium, we have the symmetry property $P(\mathbf{r}, t) = P(-\mathbf{r}, t)$, which implies that M_i vanishes for odd values of i. Note that $M_1 = 0$ is the condition for no net flow of molecules.

The diffusion coefficient in the direction $\mathbf{n}$ is defined by

$$D(\mathbf{n}) \equiv \frac{1}{2t} M_2(\mathbf{n}). \tag{1.4}$$

Extra-Cranial Applications of Diffusion-Weighted MRI, ed. Bachir Taouli. Published by Cambridge University Press.

This is the most basic diffusion metric for DWI. For normal, unrestricted diffusion $D(\mathbf{n})$ is time independent and Eq. (1.4) reduces to the well-known Einstein or Fickian relation in which position dispersion grows linearly with time, with a slope given by the diffusion coefficient[7]. Fick's law holds exactly for all regimes for an ideal liquid.

Another metric that has recently been introduced is the diffusional kurtosis defined by[8]

$$K(\mathbf{n}) \equiv \frac{M_4(\mathbf{n})}{[M_2(\mathbf{n})]^2} - 3. \tag{1.5}$$

The average of $D(\mathbf{n})$ over all directions is the mean diffusivity (MD), while the average of $K(\mathbf{n})$ over all directions is the mean kurtosis (MK).

If the diffusion moments are independent of the direction $\mathbf{n}$, the diffusion is referred to as "isotropic." Otherwise, the diffusion is referred to as "anisotropic." Some biological tissues, such as healthy liver, are isotropic to an excellent approximation, while others, such as muscle, cerebral white matter, and renal medulla, are distinctly anisotropic.

For anisotropic tissues (cerebral white matter, renal medulla, skeletal muscle), it is useful to define a diffusion tensor by[9–10]

$$D_{ij} \equiv \frac{1}{2t}\langle r_i r_j \rangle, \tag{1.6}$$

where r_i ($i = 1$, 2, or 3) is a component of the displacement vector $\mathbf{r}$. In terms of the diffusion tensor, the diffusion coefficient can be written as

$$D(\mathbf{n}) = \sum_{i=1}^{3}\sum_{j=1}^{3} D_{ij} n_i n_j, \tag{1.7}$$

where n_i is a component of the direction vector $\mathbf{n}$. Therefore, knowledge of the diffusion tensor allows one to calculate the diffusion coefficient in an arbitrary direction. The diffusion tensor can be written as a 3×3 matrix:

$$D_{ij} \equiv \begin{pmatrix} D_{11} & D_{12} & D_{13} \\ D_{21} & D_{22} & D_{23} \\ D_{31} & D_{32} & D_{33} \end{pmatrix}. \tag{1.8}$$

From the definition of the diffusion tensor, one can show that $D_{21} = D_{12}$, $D_{31} = D_{13}$, and $D_{32} = D_{23}$. The diffusion tensor is thus a symmetric matrix with 6 adjustable degrees of freedom. A spatially resolved technique that measures the full diffusion tensor in each voxel of an image is called diffusion tensor imaging (DTI).

An important property of symmetric matrices is that they can be diagonalized. This means that it is possible to rotate to a coordinate system in which the off-diagonal matrix elements vanish. In such a special or "principal" coordinate system, the diffusion tensor takes the form

$$D_{ij} = \begin{pmatrix} \lambda_1 & 0 & 0 \\ 0 & \lambda_2 & 0 \\ 0 & 0 & \lambda_3 \end{pmatrix}. \tag{1.9}$$

The three elements along the diagonal are the diffusion tensor eigenvalues and correspond to the diffusion coefficients along the coordinate axes of the principal coordinate system.

These eigenvalues play a central role in the analysis of DWI data for anisotropic tissues. The MD can be calculated from

$$\mathrm{MD} \equiv \bar{D} = \frac{1}{3}(\lambda_1 + \lambda_2 + \lambda_3). \tag{1.10}$$

The notation $\bar{D}$ for the MD is sometimes preferred for mathematical equations, since MD could be mistaken for the product of two quantities. Similarly, the "fractional anisotropy" (FA) can be calculated from

$$\mathrm{FA} = \sqrt{\frac{(\lambda_1 - \lambda_2)^2 + (\lambda_1 - \lambda_3)^2 + (\lambda_2 - \lambda_3)^2}{2\left(\lambda_1^2 + \lambda_2^2 + \lambda_3^2\right)}}. \tag{1.11}$$

The FA varies from 0 to 1 and quantifies the degree to which a tissue is anisotropic[10].

Unit vectors aligned with the principal coordinate axes are called eigenvectors. The direction that corresponds to the largest eigenvalue (usually chosen to be λ_1) is called the axial or parallel direction, while the other two directions are called the radial or perpendicular directions. This is because the source of anisotropy is often the presence of fibrous structures, as in muscle or renal tubules, which restricts diffusion more strongly in directions perpendicular to the fibers. The axial diffusivity is given by

$$D_{\parallel} \equiv \lambda_1, \tag{1.12}$$

and the radial diffusivity is given by

$$D_{\perp} \equiv \frac{1}{2}(\lambda_2 + \lambda_3). \tag{1.13}$$

By construction, $D_{||} \geq D_{\perp}$. Also note that from Eqs. (1.10), (1.12), and (1.13), we find the identity $\bar{D} = (D_{||} + 2D_{\perp})/3$.

For simple aqueous solutions, the diffusion process is well described by the isotropic, Gaussian distribution:

$$P(\mathbf{r}, t) = \frac{1}{(4\pi Dt)^{3/2}} \exp\left(-\frac{|\mathbf{r}|^2}{4Dt}\right). \quad (1.14)$$

For this distribution, one can show that FA = MK = 0. However, in biological tissues, diffusion restrictions, such as cell membranes, may cause $P(\mathbf{r}, t)$ to deviate significantly from this canonical form. For isotropic tissues, we still have FA = 0, but MK will typically have a positive value. In fact, the MK is constructed precisely to be an index for the degree to which the diffusion process is non-Gaussian, and as such, it may be regarded as an indicator of tissue microarchitectural complexity (i.e., the diffusion restrictions). An MK value of around 1 or higher implies a significant degree of diffusional non-Gaussianity. For anisotropic tissues, the FA will be positive, as well. We emphasize that there is no simple connection between the FA and the MK, so that these two metrics provide complementary information about water diffusion in tissues. In analogy with DTI, an imaging protocol that produces maps of diffusional kurtosis metrics (e.g., MK) is termed diffusion kurtosis imaging (DKI).

In principle, diffusion metrics, such as $D(\mathbf{n})$ and $K(\mathbf{n})$, have a time dependence in complex media such as biological tissues. This time dependence is typically strongest when the diffusion length is comparable to characteristic length scales of the media. The diffusion length is defined as

$$l_D \equiv \sqrt{6\bar{D}t} \quad (1.15)$$

and corresponds to the root-mean-square distance that a molecule moves during an observation time t (often called the diffusion time). For biological tissues, the MD for water is typically about 1 μm^2/ms, and for DWI, the diffusion times are typically about 50 ms. This gives a diffusion length of about 17 μm, which is indeed comparable to cell sizes. Thus some dependence of diffusion metrics on the diffusion time may be expected and care should be taken when comparing diffusion measurements obtained with different diffusion times. In most cases studied in the brain[11–12], diffusion time dependence has been found to be relatively modest over the normal range of diffusion times (20 to 80 ms), although it is more pronounced over longer diffusion times[13].

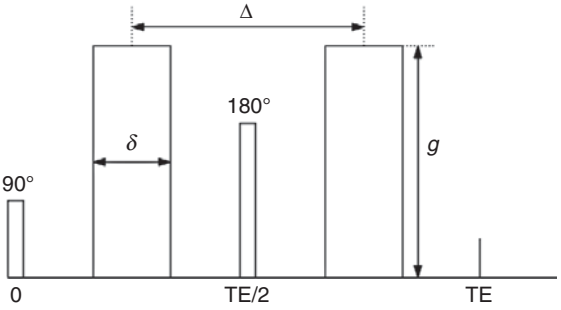

Figure 1.1 The Stejskal–Tanner sequence has been commonly used for DWI. It consists of a conventional spin echo sequence with one diffusion sensitizing gradient lobe inserted between the initial 90° excitation pulse and 180° refocusing pulse and with another inserted between the 180° pulse and the signal readout at the echo time (TE). The interval between the centers of the diffusion gradient lobes corresponds to the diffusion time (Δ). The strength of the diffusion weighting (i.e., the *b*-value) depends on the magnitude (g) and duration (δ) of the diffusion gradients, as well as the diffusion time, according to Eq. 1.17 (See text).

So far, we have considered molecular diffusion without reference to how it is measured with NMR or MRI. To illustrate the concepts underlying diffusion measurement, let us consider the famous Stejskal–Tanner sequence[3–4]. The key element of this sequence is the pair of strong gradient lobes that sensitize the signal to molecular diffusion. These "diffusion gradients" are balanced and so have no effect on the signal magnitude if the molecular spins (i.e., water protons) are stationary. But the diffusion gradients cause measurable signal loss for even the small amount of motion associated with molecular diffusion. The diffusion direction corresponds to the orientation of the diffusion gradients. A pulse diagram for the Stejskal–Tanner sequence is shown in Fig. 1.1.

If one applies this sequence to a media with Gaussian diffusion, the signal intensity is given by

$$S(b) = S_0 e^{-bD}, \quad (1.16)$$

where S_0 is the signal intensity in the absence of diffusion gradients, D is the diffusion coefficient in the direction of the diffusion gradients, and

$$b \equiv (\gamma \delta g)^2 \left(\Delta - \frac{\delta}{3}\right). \quad (1.17)$$

This defines the so-called *b*-value. Here γ is the gyromagnetic ratio (equal to 2.675×10^8 s^{-1}/Tesla for

water protons), g is the magnitude of the diffusion gradients, Δ is the diffusion time, and δ is the pulse duration. For arbitrary pulse sequences the b-value can be calculated from the effective gradient waveform G_{eff} according to the more general formula[14]

$$b = \gamma^2 \int_0^{TE} \left[\int_0^t g_{eff}(t')dt' \right]^2 dt \qquad (1.18)$$

Here g_{eff} reflects the effective diffusion-weighting gradient including the phase reversal effects of radiofrequency pulses in the sequence. Furthermore, in some cases the diffusion-weighting effect of the imaging gradients must also be taken into account for maximal accuracy[15]. For clinical DWI of the brain, b-values typically range from zero to several thousand s/mm^2. For body imaging, b-values usually are not much more than 1000 s/mm^2 due to shorter T2 times limiting signal-to-noise ratio.

Since Eq. (1.16) has two unknown parameters, the diffusion-weighted signal must be measured for at least two different diffusion weightings (i.e., b-values) in order to determine D. If exactly two b-values are used, then one has the simple formula

$$D = \frac{1}{b_2 - b_1} \ln\left[\frac{S(b_1)}{S(b_2)}\right]. \qquad (1.19)$$

Although Eq. (1.16) is the basis of most analyses of DWI data, one should be aware that it is only exact for Gaussian diffusion, while diffusion in biological tissues may be significantly non-Gaussian. Indeed, departures from the monoexponential form of Eq. (1.16) can be used to estimate the MK[8].

Even when Eq. (1.16) appears to be a good fit to experimental data, measured values for D may still depend to some extent on Δ and δ, as well as the echo time, due both to the effect of diffusion restrictions and intravoxel variations in T2 values[12]. Therefore, it is best practice to be consistent with the selection of these parameters.

Strictly speaking, diffusion refers to random molecular motion. However, in biological tissues, blood flow through the capillary network can mimic diffusion and will affect measured diffusion metrics obtained with DWI. This effect is referred to as intravoxel incoherent motion (IVIM). The essential idea is that the capillary network can have a quasi-random arrangement so that flow through the capillaries (and other small blood vessels) leads to random movement of blood referred to as pseudo-diffusion[16–17].

When IVIM is significant, then the diffusion signal is more accurately modeled by the biexponential form

$$S(b) = S(0)\left[f_p e^{-bD^*} + (1 - f_p)e^{-bD_t}\right], \qquad (1.20)$$

where D_t is the tissue diffusion coefficient, D^* is the pseudo-diffusion coefficient for blood, and f_p is the blood volume fraction (a.k.a. "perfusion fraction"). In practice, f_p more precisely refers to the relative water fractions of the blood compartment, since DWI is normally measuring water diffusion.

As Eq. (1.20) suggests, the IVIM effect tends to be large in organs with a high blood volume, such as liver and kidney[17–18]. Pseudo-diffusion coefficients are typically many times larger than tissue diffusion coefficients[17], and the second term of Eq. (1.20) is often negligible for b-values above 300 s/mm^2. If the IVIM effect is substantial, but DWI data are fit to Eq. (1.16) rather than Eq. (1.20), then diffusion coefficient estimates may depend significantly on the choice of b-values.

In part due to IVIM, a diffusion coefficient estimate obtained with DWI became known as an apparent diffusion coefficient (ADC) to remind us that it may be influenced to some degree by effects other than true molecular diffusion. Logically, one may also include the aforementioned dependences of D on pulse duration, intravoxel T2 variations, and non-Gaussian diffusion response as justifications for the moniker "apparent." ADC is used to refer both to D in a given direction and to the MD, although mean diffusivity is preferred for the latter.

In fact, modifications to "apparent" water diffusion due to structural restriction have proven to be a more pervasive MRI contrast mechanism than active flow-induced IVIM. Water embedded in biological media (cells, axons, tubules, blood vessels) undergoes more complex hindered, restricted, or driven motion. However, the average diffusion moments of the whole spin ensemble are still useful descriptors and serve as biomarkers of the tissue structure. To first approximation, diffusion in tissue (and more generally in porous media[19]) obeys Fick's law with a reduced ADC. For isotropic tissues, it suffices to measure diffusion in a single direction, and one often may be primarily interested in determining the ADC. For anisotropic tissues, multiple diffusion directions are

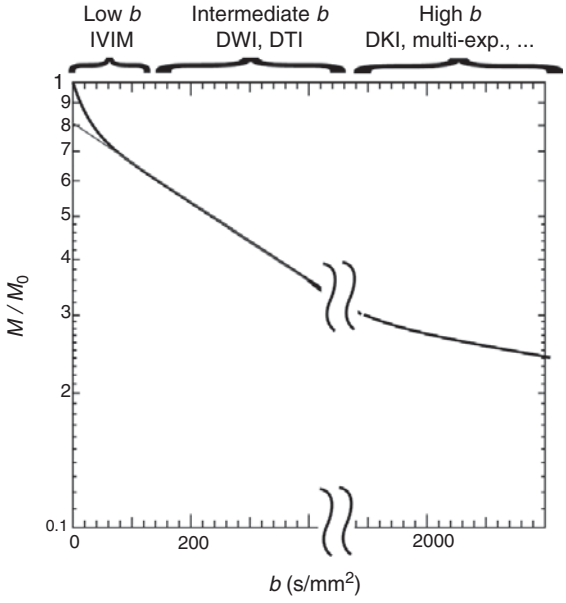

Figure 1.2 Sketch of diffusion-weighted signal decay behavior in several regimes of diffusion-weighting for in vivo tissue response.

required to fully characterize the diffusion process. In particular, in order to estimate the diffusion tensor, at least six directions are needed since the diffusion tensor has six adjustable parameters. However, if only the MD is required, then it can be found from the average of ADCs measured for any three orthogonal directions.

Experimentally, the various effects just described can be organized according to the regimes of diffusion weighting in which they are observed to occur (Figure 1.2). The low b-value regime ($0 < b < 200$ s/mm^2) is where pseudo-diffusion from microcirculation effects are found (i.e., the IVIM regime), since pseudo-diffusivities are typically quite high ($D^* \sim 10 - 50$ mm^2/ms). Studies wishing to avoid vascular contamination typically exclude this range; conversely, those aiming to quantify vascularity with DWI may sample both this regime and the normal diffusion regime heavily. The mostly commonly used regime is the intermediate regime ($200 < b < 1000$ s/mm^2), where diffusion appears Gaussian and DWI signal decays appear monoexponential. In this regime, standard DWI metrics (e.g., ADC) or DTI metrics (MD, FA, eigenvalues) are typically derived. Finally, the high b-value regime ($b > 1000$ s/mm^2) also often shows non-monoexponential signal decay due to microscopic parenchymal structure, which can be quantified for example with diffusional kurtosis. In clinical scanners, the b-value is typically incremented by adjusting diffusion gradient magnitude g, or equivalently the diffusion wave vector $q = \gamma g \delta$, the inverse of one of the probing length scales of DWI. At high b-values, q^{-1} is comparable to or shorter than parenchymal length scales of a few microns (cell size, axon radius, membrane thickness) and their geometry begins to manifest in a non-monoexponential signal decay[20–21]. Depending on the organ, pathology, data sampling, and precision, one can model this behavior in different ways (either with physical models or empirical descriptions) to extract microstructural markers. Example models include multiexponential functions reflecting tissue compartments[21–23] (similar to the IVIM vascular/parenchymal decomposition), the cumulant expansion model which extracts higher-order displacement moments[8,24–25], or other models of tissue complexity[26–27]. In all cases, the model and interpretation must be chosen with regard to the data precision and tissue prior knowledge; compartmental models for example can be overinterpreted since multiexponentiality does not necessarily equate to compartmentalization[28–29]. These issues will be further discussed below.

1.3 DWI techniques

Pulse sequences (Figures 1.3 and 1.4)

The desired contrast in DWI is an attenuation of the *magnitude* of the spin magnetization following the diffusion-weighting gradient waveform due to microscopic incoherent motion, as described in Sections 1.1 and 1.2. However, macroscopic motion such as respiration, pulsation, or bulk translation/rotation can induce *phase shifts* in the spin magnetization which can be temporally and spatially heterogeneous. In MRI sequences with segmented k-space trajectories, these motional phases can induce phase inconsistency across k-space and therefore image ghosting. For this reason, particularly for body applications, the most common modalities for DWI are single-shot sequences. Also, the magnitude channel is retained and the phase channel is typically discarded. Two examples are echo-planar imaging (EPI)[30] and turbo spin echo (TSE)[31] imaging (see Figure 1.3 for pulse sequence diagrams).

Echo-planar imaging (EPI)

Echo-planar imaging (EPI)[30] is one of the mainstay techniques for fast MRI, and is the key to such

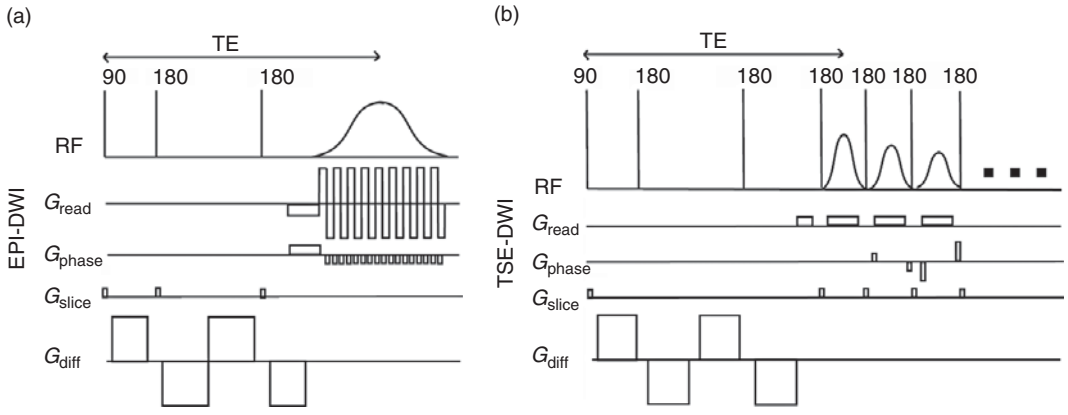

Figure 1.3 DWI single-shot pulse sequence diagrams. (a) Echo-planar imaging (EPI). (b) Turbo spin echo (TSE).

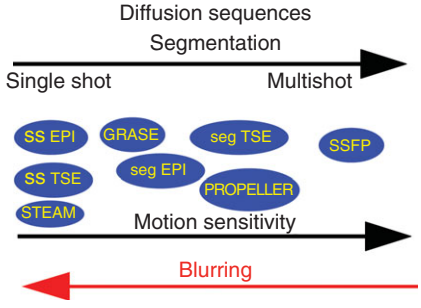

Figure 1.4 Diffusion imaging strategies as a function of *k*-space segmentation. In general, more segmentation reduces image blurring but requires motion correction, and vice versa.

powerful applications as functional imaging (fMRI), diffusion tensor imaging (DTI), and perfusion-weighted imaging (PWI). For DWI, it is most often run in 2D single-shot mode, where all the required lines of acquisition (*k*-space) for a 2D spatial slice are all collected in an echo train following a single excitation and diffusion weighting preparation. For full-body human clinical MRI scanners, the standard implementation of the diffusion-weighting preparation is a twice-refocused spin echo with bipolar gradients, as depicted in Figure 1.3a, which has the advantage of eddy-current compensation for improved image quality[32]. A disadvantage of this approach is a longer required echo time (TE) for the same diffusion weighting factor (*b*) in comparison with a simpler Stejskal–Tanner sequence. While some aspects of this technique carry over smoothly from cerebral to abdominal imaging, other challenges are unique to the abdominal setting and require modifications of the imaging paradigm.

The EPI echo train is collected within the envelope of a single spin echo MR transient, and so suffers attenuation due to intravoxel static magnetic field inhomogeneity (characterized by a spatially dependent time constant T_2^*) as well as phase shifts from the average local field deviations. The former effect induces blurring in the image, while the latter induces distortions, and both are generally referred to under the category magnetic susceptibility artifact. Both can be particularly problematic in abdominal DWI, given the heterogeneous adjacent organs (liver, kidney, spleen), some of which contain air (bowel, stomach, lung). Therefore, measures are taken to reduce the echo train length (ETL) as much as possible. One example is partial Fourier, where as little as half the full *k*-space is collected and combined with assumptions of phase symmetry is sufficient to generate an image[33]. Another solution, which is very common for body MRI[34–36], is the use of parallel imaging undersampling, where spatially varying receiver coil sensitivity information is used in lieu of full *k*-space sampling for image reconstruction. Each of these solutions reduces ETL and thus blurring and distortions, but in exchange for lower SNR due to fewer-acquired data and/or the processing cost of coil-based reconstruction.

For further image quality improvement, segmented *k*-space trajectories where far fewer lines (5–10) are acquired in a single excitation have been used with EPI-DWI[37–38]. Since motional phase errors can induce inconsistency among segments, navigator echoes (with 1D, 2D, or even 3D phase mapping) are required to prevent ghosting in these segmented EPI-DWI sequences[39–40]. For single-shot sequences, even if

individual image quality is uncorrupted, the entire image set must be positionally consistent prior to diffusion processing, particularly for the diffusion tensor. During acquisition, physiological triggering (respiratory gating[41–42] or pulse triggering[43]) is employed to minimize bulk motion. Physiological triggering can use signals from either patient devices (finger pulse sensor, abdominal pad/belt transducer) or from simultaneous MR navigation (e.g., of diaphragm motion). When possible, breath-hold acquisitions are performed to minimize patient motion during the acquisition, though usually at the expense of some SNR due to suboptimal repetition times TR. Finally, even in gated or breath-hold acquisitions, post-acquisition registration is often needed to completely align the dataset prior to diffusion processing.

Most clinical abdominal EPI-DWI has been performed at 1.5 T, but 3-T applications are becoming more common[44–47]. The advantage of higher raw SNR at higher field must be considered in balance with the larger susceptibility artifact, and shorter transverse relaxation time T2[48]. Parallel imaging, which generally becomes more favorable at higher field, is one potential solution to these issues.

Turbo spin echo (TSE)

The second most common single-shot diffusion-weighted imaging sequence uses a turbo spin echo (TSE) readout, also known as fast spin echo (FSE) or rapid acquisition with relaxation enhancement (RARE). This sequence, depicted in Figure 1.3b, employs a train of spin echoes generated by a series of 180° refocusing pulses, each of which provides one line of *k*-space, similar to the EPI gradient echo train. Importantly, however, the spin echo-based TSE signals are insensitive to susceptibility-induced blurring and distortions. Accordingly, the limiting signal envelope is determined not by the total transverse relaxation time T_2^* but by the usually longer irreversible transverse relaxation time T_2; thus TSE images can show "T2-blurring." The temporal advantage is somewhat mitigated by the time required for slice-selective inversion pulses between each echo, but TSE images are in general more morphologically accurate than EPI counterparts.

Other artifacts are unique to the DW-TSE protocol. The most important one arises due to the essentially random phase imparted to the magnetization following diffusion-weighting, but before TSE readout, due to bulk motion. This phase causes the (Carr–Purcell–Meiboom–Gill) CPMG condition[2,49], which usually provides for echo pathway isolation and also RF pulse error compensation, to be violated. This effect, especially when combined with RF pulse errors generating unwanted stimulated echo pathways, causes interference between the desired signal parity and spurious signals of opposite parity[31,50]. This "non-CPMG" artifact manifests as streaking or banding roughly perpendicular to the frequency-encoding axis, and is regionally pronounced in areas of RF or B0 inhomogeneity. Various solutions have been implemented, including spoilers to isolate desired parity[50], split-echo techniques to separately acquire both parities and combine them offline[51–52], and phase modulations to stabilize both signals' phase histories[53].

Like EPI, the TSE echo train can include complete *k*-space coverage (single-shot mode) or only portions in each excitation (segmented mode); with diffusion-weighting preparation, the segmented protocol must be accompanied by navigator echo collection to correct intershot motional phase errors[54]. Some strategies solve this problem by using self-navigated radial trajectories that pass through the center of *k*-space often, allowing measurement and correction of motional phases. Segmented radial TSE sequences such as PROPELLER[55] (a.k.a. BLADE) have had great success in DWI in both the brain and body[52,56–57].

Regarding field strength, TSE-DWI is also progressively migrating to the higher field platform (e.g., 3 T) for body imaging[58]. Unlike EPI, TSE does not suffer increased distortion at higher field and therefore may be preferred in regions of high susceptibility contrast (lung, breast, etc.). However, the refocusing RF pulse train will give rise to higher specific absorption rate (SAR) due to the higher Larmor frequency at higher field, so RF heating restrictions may extend scan time.

Other pulse sequences

GRASE and STEAM

We have seen that EPI generates gradient echo trains with rapid gradient reversals, and TSE generates spin echo trains with rapid refocusing RF pulses. In some cases hybrid methods employing both gradient and spin echo (GRASE) signals to accelerate *k*-space have also been used for diffusion imaging[57]. Another approach is a stimulated echo acquisition mode (STEAM), in which a series of stimulated echoes

(STE) are generated by two 90° pulses followed by a train ("burst") of low-flip angle pulses, each one "stimulating" a portion of the stored magnetization from the first pulse pair[59–60]. Since each STE is "fresh" from storage mode there is no blurring due to susceptibility or transverse relaxation. However, the STEAM–BURST pulse train progressively depletes the stored magnetization as *k*-space is acquired, which dictates lower SNR signals and in some cases RF demodulation corrections. STEAM preparation can also be used followed by another readout (EPI or SSFP)[61–62], which has advantages for more specific quantification of tissue microstructure when the diffusion time is a control variable.

Steady-state free precession (SSFP)

The limit of a fully segmented acquisition, i.e., one *k*-space line per excitation, induces minimum blurring, but maximum motion artifacts and, if full recovery were allowed between lines, maximum acquisition time. One solution to this problem is to use steady-state-free-precession (SSFP) sequences that include diffusion weighting[63–66]. These sequences employ a rapid train of excitations that do not allow full magnetization recovery but instead arrive at a lower driven equilibrium "steady state" value. The reduced magnitude is more than compensated by acquisition speed in overall scan efficiency. Though slower than single-shot modes (inter-signal spacing is TR ~ 30–50 ms), SSFP allows in principle very high quality diffusion imaging in acceptable time-frames. However, there are two complications to this technique which have thus far mostly confined its successful use to the brain. First, as mentioned above, segmentation requires motion correction. In this case, every line must be accompanied by a navigator signal, ideally a multidimensional one to capture non-uniform motion[66–68]. Second, the diffusion-weighting of the SSFP signal is "entangled" in a complicated way with effects of relaxation weighting and RF flip angle excitation[63,69]; thus, successful quantitation requires not only multiple diffusion weightings for good-quality curve fitting, but also prior knowledge or separate maps of relaxation times T1, T2, and RF field B1. Thus, SSFP diffusion imaging potentially provides maximum quality and resolution, but at a high price in navigation and peripheral acquisitions. For abdominal applications it may only apply to relatively immobile organs like the prostate. Alternatively, SSFP can be used as a pure readout modality following a more standard diffusion preparation[70].

1.4 Data analysis

Once a set of DWI images has been obtained, one would then normally like to use them to generate parametric maps of various diffusion metrics. This requires a certain amount of post-processing, the details of which can be fairly complicated. Here, we give a general overview of some of the key considerations, while trying to minimize mathematical formalities. A more in-depth description for one particular image analysis program for DWI is given by Jiang and co-workers[71].

Raw diffusion-weighted images themselves are sometimes considered clinically informative, but it should always be remembered that the observed contrast depends strongly on additional, non-diffusion-related factors such as relaxation rates and proton density. The so-called "T2 shine-through" effect is perhaps the best-known example of this problem[72].

In order to obtain pure diffusion maps, the first step is often to co-register the DWI images to correct for any relative displacements or rotations due to patient motion. This is important, because the images are processed as a set and misregistration between images can lead to significant artifacts and alter estimates of the ADC and other quantities. A variety of image analysis programs are available that can perform the necessary co-registration. However, image co-registration may not always be necessary for certain organs, such as prostate, where motion can be minimal. Alternatively, if gating strategies have been used in the acquisition process as discussed earlier, then some physiological motion will have been minimized.

Once co-registered, the images can be used to calculate the desired diffusion metrics on a voxel-by-voxel basis, yielding parametric maps. The most widely employed diffusion maps are for the MD and FA, although the axial and radial diffusivities are gaining popularity[73].

A useful extension of the FA map is called the FA color or directivity map[74]. Here each pixel of an FA map is converted to red–green–blue (RGB) color by using the eigenvector corresponding to the highest eigenvalue, which in many cases may be reasonably assumed to be oriented parallel to any fiber-like structures. The intensity of the red is determined by the FA multiplied by the *x*-component of the eigenvector

in a specified reference frame, while the green and blue intensities are determined by products of the FA with the y- and z-components. In this way, a directivity map displays both the degree of anisotropy as well as the orientation of the fibers.

An alternative approach for displaying diffusional anisotropy is to perform fiber tracking (FT), which is again based on an assumption that fibers are the source of anisotropy. An FT algorithm generates trajectories, originated from a set of selected starting points (seeds) and guided by using the primary eigenvector field to trace streamlines that are intended to show the fiber paths within a tissue. This method has been used extensively for mapping white matter tracts within the brain and has also been applied to study muscle[75] and kidney[76].

In the brain, the IVIM effect is small and usually ignored in the analysis of DWI data. In body, however, the IVIM effect can be much more significant and may have to be taken into account[17–18]. As previously mentioned, a typical indication of an IVIM effect is finding ADC values that depend on the choice b-value, when a conventional monoexponential model is used to fit the signal data.

In such cases with a large IVIM effect, it can be useful to fit to the biexponential model of Eq. (1.20), provided DWI data is available for a sufficient range of b-values. Since Eq. (1.20) has four unknown parameters, one needs data for at least four different b-values. Ideally, two of these would be for $b < 200$ s/mm^2, as the IVIM effect is mainly important for low b-values. Great care should be taken when performing the fit due to the sensitivity of the fit parameters to noise[77–78]. Sometimes more robust results can be obtained by a "segmented" procedure of first fitting the high b-value (i.e., $b > 300$ s/mm^2) data to a monoexponential to determine f_p and D_t, and then fitting to Eq. (1.20) with D_t fixed to this predetermined value.

As an example, consider a set of DWI measurements for the four b-values: 0, $b_1 = 150$ s/mm^2, $b_2 = 500$ s/mm^2, $b_3 = 1000$ s/mm^2. If it is assumed that the IVIM effect is negligible for $b > 300$ s/mm^2, one can then estimate

$$D_t = \frac{1}{b_3 - b_2} \ln\left[\frac{S(b_2)}{S(b_3)}\right]. \tag{1.21}$$

From this result, one can in turn determine the other parameters for the biexponential model by using the formulae

$$f_p = 1 - \frac{S(b_3)}{S(0)} e^{b_3 D_t}, \tag{1.22}$$

$$D^* = -\frac{1}{b_1} \ln\left[\frac{S(b_1)}{f_p S(0)} - \frac{(1 - f_p)}{f_p} e^{-b_1 D_t}\right]. \tag{1.23}$$

Since the signal intensity of diffusion-weighted images drops sharply with increasing b-value, noise is often an important source of error in the analysis of DWI data. Unless noise is explicitly modeled in the data fits, then the maximum b-value that can be used without causing significant errors in estimated diffusion metrics depends both on the intrinsic SNR (i.e., without diffusion weighting) and the ADC. This maximum b-value is approximately given by[79]

$$b_{\max} \approx \frac{1}{D} \ln\left(\mathrm{SNR} \cdot \sqrt{\frac{2}{\pi}}\right). \tag{1.24}$$

After maps of diffusion metrics have been obtained, then mean values for different regions of interest are usually compared. For large regions of interest, containing many voxels, histogram approaches, such as principal component analysis, may be useful[80–81].

1.5 Body applications

The biophysical mechanisms affecting diffusion weighted imaging in the body, reviewed in previous sections, have a wide range of applications in abdominal imaging. Many pathological mechanisms involve alterations in the parenchymal structure that affect the natural scale or shape of restrictions/hindrances to water motion (cell membranes, sheaths, fibers, tubules, etc.). Others are sensitive to changes in fluid content, such as in cysts, edema, or glandular compartments, as well as desiccation. Finally, the IVIM methodology can reveal changes in the abundance or flow speed (or both) of tissue vascularity. The impacts of these sensitivities are itemized below in several abdominal organ categories, following a few brief comments about common tissue states or pathologies.

Common entities (Table 1.1)

Certain entities are common to multiple organs and/or pathologies. Edema, or abnormal fluid release surrounding pathological insults to tissue such as carcinoma or injury, tends to increase apparent diffusion coefficients (i.e., ADC, MD, or D_t). Simple cysts are isolated pockets of free fluid that show normal

Table 1.1 Typical changes in diffusion MR metrics with common tissue entities

	ADC/MD/D_t	FA	MK	f_p	D_p
Edema	↑	↓	↓	0	NA
Cyst	↑	0	0	0	NA
Fibrosis	↓	↓	↑	0	NA
Tumor	↓	↓	?	↑	↓

Notes: ADC: apparent diffusion coefficient; MD: mean diffusivity; D_t: tissue diffusivity; FA: fractional anisotropy; MK: mean kurtosis; f_p: perfusion fraction; D_p: pseudo-diffusivity.

unrestricted diffusion (high ADC), while complex cysts may show a mixture of free fluid and hemorrhagic fluid, the latter of which shows slower diffusion due in part to higher viscosity. Fibrosis, or an abnormal growth of fibrous parenchymal tissue, increases the prevalence of barriers to diffusion and thus reduces ADC values and would be expected to increase diffusional kurtosis.

Finally, tumors possess several properties for which diffusion imaging can provide biomarkers. First and foremost, the proliferation of cancer cells generally reduces the extracellular space and thus the ADC by an amount depending on aggressiveness. Thus, the ADC is considered a marker of the "cellularity" of malignant tumors throughout the body. While diffusion in the aggressive tumor core is usually isotropic (FA ~ 0), high resolution DTI of brain tumors has revealed significant diffusion anisotropy in the infiltration rim zone, corresponding to either radial or azimuthally oriented cell patterns[82–83]. Diffusional kurtosis can be either higher or lower in tumors than normal tissue. Most tumors (with a few notable exceptions) are hypervascular due to unregulated angiogenesis. This effect generally promotes the IVIM pseudo-diffusion effect in DWI; indeed, a monoexponential model can potentially confuse effects of vascularity and cellularity since they have opposite influences on apparent diffusion. When analyzed properly with an IVIM compartment model, tumors usually display higher perfusion fraction (f_p) than background tissue, and sometimes abnormal pseudo-diffusivity (D_p) for sluggish blood flow. These effects are common to many tumor types but differences exist in the diffusion measurement and interpretation of each organ separately.

Liver

Hepatic tissue possesses several properties in health and disease that diffusion imaging can probe[84]. First, hepatic tissue is highly vascular, which translates to a high IVIM perfusion fraction ($f_p \sim 30\%$)[17–18,85]; accordingly, studies have observed dependencies of ADC results on selected *b*-values[86]. Compared to other organs, the liver has a short transverse relaxation time T2[48] (and significantly more so in the case of iron overload[87–88]) and thus reduces available SNR for diffusion imaging. Secondarily, sufficient iron deposition can generate local magnetic field inhomogeneities that can interfere with applied gradients and thus alter prescribed *b*-values. Liver fibrosis and cirrhosis is a prominent pathology in which DWI has been shown to have significant diagnostic potential[17,85,89], since cirrhosis is thought to involve both vascular (reduced flow) and parenchymal (fibrotic growth) abnormalities. Figure 1.5a shows example images of total apparent diffusion coefficient (ADC_{tot}), tissue diffusivity (D_t), and perfusion fraction (f_p) in a healthy and cirrhotic patient from IVIM MRI performed at 1.5 T (taken from[89]). All three parametric maps show differences between the two subjects, consistent with multifactorial pathophysiology of cirrhosis. Such information updates previously held convention that diffusion contrast in cirrhosis reflected only fibrotic restriction. Finally, hepatocellular carcinoma (HCC) is a significant health threat in which MRI plays a key role in detection and diagnosis. High cellularity in the tumor zone reduces ADC values, and high vascularity has also been shown to demonstrate high perfusion fractions in IVIM studies[18].

Kidney

The two tissue types in renal parenchyma, cortex and medulla, can be tracked by DWI via several physiological properties: vascular flow, tubular flow, and parenchymal structure. As the kidney is one of the most highly vascularized bodily organs, blood volume and blood flow are significant contributors to overall water transport in the cortex and medulla, and thus a strong pseudo-diffusion component is present in IVIM imaging. Additionally, active tubular flow in both compartments is another source of pseudo-diffusion in the DWI signal. Figure 1.6 shows DWI signal decay data from cortex, medulla, and benign cyst regions of a normal healthy volunteer[90–91]. In comparison with the nearly monoexponential